Characterisation of Quorum Sensing System and Its Role in Global Regulation in *Hafnia alvei*

Jia Yi Tan[1,2], Wah-Seng See-Too[1], Peter Convey[3], Kok-Gan Chan[1,2]*

Author affiliations:
[1] Division of Genetics and Molecular Biology, Institute of Biological Sciences, Faculty of Science, University of Malaya, Kuala Lumpur 50603, Malaysia;
[2] International Genome Centre, Jiangsu University, Zhenjiang 212013, PR China;
[3] British Antarctic Survey, NERC, High Cross, Madingley Road, Cambridge CB3 OET, UK

***Correspondence**: Kok-Gan Chan, kokgan@um.edu.my

Keywords: Genomic, Transcriptomic, RNA-seq, Quorum sensing, *Hafnia alvei*

Abstract: Quorum sensing (QS) is a regulatory process achieved *via* cell-to-cell communication that involves release and detection of autoinducers (AIs), and which occurs in a wide range of bacteria. To date, QS has been associated with events of pathogenesis, biofilm formation, and antibiotic resistance in clinical, industrial, and agricultural contexts. The main objective of this study was to characterise the role of *N*-Acyl homoserine lactone (AHL) type QS in *Hafnia alvei* FB1, a bacterial strain isolated from frozen vacuum-packed fish paste meatballs, via identification of QS core genes using a genomic approach, followed by comparative transcriptomic profiling between QS-deficient mutants and wild-type strains. *H. alvei* FB1 is known to produce two types of AHLs, namely, *N*-(3-oxohexanoyl) homoserine lactone (3OC6-HSL) and *N*-(3-oxooctanoyl) homoserine lactone (3OC8-HSL). The complete genome sequence of strain FB1 was obtained and a single gene for AHL synthase (*halI*) and its cognate receptor (*halR*) were identified. QS-deficient mutants of FB1 were constructed via the λ-Red recombineering method. Removal of the QS genes in strain FB1 affected mainly mechanisms in cell division and nutrient uptake, as well as resistance to a number of antibiotics, which are crucial for survival, adaptation and colonisation of both food and the host gut environment.

Importance: Members of the genus *Hafnia* are known as opportunistic pathogens in both nosocomial and community-acquired infections. However, the involvement and mechanism of pathogenesis of *Hafnia* in infectious diseases remains uncertain. We investigatd the role of the signalling molecule group, *N*-acyl homoserine lactones (AHLs), in a *Hafnia alvei* strain, since AHLs play important roles in pathogenicity, survival or adaptation in other pathogens. The comparative transcriptomic study revealed that AHLs are involved in mechanisms in cell division and nutrient uptake, as well as resistance to a number of antibiotics, which are crucial for survival, adaptation and colonisation of both food and the host gut environment. These findings provide insight into possible strategies to combat this opportunistic pathogen.

Data summary: Genome sequence is deposited in NCBI GenBank under accession number CP009706. The transcriptomic data have been deposited in the Gene Expression Omnibus (GEO) database (https://www.ncbi.nlm.nih.gov/gds) under accession number GSE93000.

Introduction

Quorum sensing (QS) is a form of cell-to-cell communication expressed by a wide range of bacterial species, achieved by the release and detection of signaling molecules called autoinducers (AIs) (1). *N*-acyl-homoserine lactone (AHL) is one such type of molecule, commonly produced by Proteobacteria. Individual cells monitor the changes in 'quorum' through detection of these small, often lipophilic, molecules in the environment and, in response, adjust the expression of a network of genes in a collective manner (2). AHL-based QS has been reported to be associated with various microbial activities of clinical, industrial, and agricultural importance, such as regulation of virulence expression (3-5), production of antibiotics (6, 7), biofilm formation (8-10), and food spoilage (11-13).

Hafnia, a bacterial genus characterised by rod-shaped, motile, flagellated and facultatively anaerobic cells, belongs to the family *Hafniaceae*. *Hafnia alvei* has been identified to be among the enteric bacteria commonly involved in food spoilage (11, 12, 14, 15), and also as an opportunistic pathogen (16). The ability of *H. alvei* to survive at low temperature (15) has made it an interesting subject of study in controlling bacterial contamination in the food industry. Despite the common association of *H. alvei* with human gut microbiota (17-19), its status as a gut pathogen is still uncertain. Therefore, it is also important to confirm whether this common microbial contaminant of food could also be a source of gut infection.

The focus of this study, *H. alvei* FB1 is an AHL-producing strain recovered from vacuum-packed refrigerated fish paste meatballs (commonly known as 'fish ball'). We have previously confirmed that the strain produces two oxo-AHLs with side chains of six or eight carbons in length (20).

In recent years, advancement in high-throughput sequencing and accessibility of powerful bioinformatics pipelines have enabled bacterial genomes and transcriptomes to be explored with increasing ease. Further, current DNA recombinant technology allows precise genome editing and provides a convenient tool in the study of QS regulons. This study investigated the genetic basis of AHL-based QS signalling in *H. alvei* FB1, as well as the regulatory role of QS in *H. alvei,* by studying the QS-deficient mutants in a comparative transcriptomics context.

Methods

Bacterial Strains, Plasmids and Culturing Conditions

All bacterial strains and plasmids used in this study are listed in Table 1 along with their relevant characteristics. All strains were cultured and maintained in Luria-Bertani (LB) medium. Unless stated otherwise, the growth temperatures for *Chromobacterium violaceum* CV026, *Escherichia coli* and *H. alvei* strains were 28°C, 37°C and 30°C, respectively.

Whole Genome Sequencing

92 The gDNA used in this study was extracted with the MasterPure™ DNA Purification Kit
93 (Epicentre, USA) following the manufacturer's protocol. The quality of gDNA extracted was
94 assessed according to "PACBIO® GUIDELINES FOR SUCCESSFUL SMRTbell™ LIBRARIES" prior
95 to library preparation for sequencing. Preparation of SMRTbell template libraries was carried
96 out with SMRTbell Template Prep Kit 1.0 (Pacific Biosciences, USA) following the
97 manufacturer's protocol for 20 kb template preparation. SMRT sequencing was performed
98 using a PacBio RSII Sequencer (Pacific Biosciences, USA) with 3 SMRT cells.
99
100 Quality filtering and *de novo* assembly of the output reads were performed using the
101 Hierarchical Genome Assembly Process (HGAP) pipeline version 3.0 on the Pacific Biosciences'
102 SMRT portal (21). Polished assemblies were generated from this module that incorporated
103 Celera Assembler, BLASR mapper, and Quiver consensus caller algorithms. The assembled
104 genome sequence was then annotated by SEED-based subsystem characterisation on the
105 RAST server (22, 23) and Prokaryotic Genome Automatic Annotation Pipeline (PGAAP) (24).
106
107 **Identification of QS genes from the annotated data**
108
109 Candidates of potential *luxI* and *luxR* homologues were identified from the annotated
110 genome with the 'BLAST search' function on RAST. A search on the Conserved Domain
111 Database (CDD) (25) was performed to identify the signature conserved domains on the
112 candidate sequences. The sequences were aligned with other known homologues obtained
113 from the GenBank database (https://www.ncbi.nlm.nih.gov/) and visualised using Jalview
114 version 2. Phylogenetic analysis was performed using SeaView version 4 (26).
115
116 **Cloning and Expression of the *luxI* homologue**
117
118 Identity and function of the *luxI* homologue were determined via cloning and expression
119 study using Gene Synthesis service (GenScript, USA). The target DNA sequence was first
120 synthesised in vector pUC57, and then sub-cloned into *E. coli* expression vector pGS21a by
121 the service provider. The expression vector carrying the target sequence was transferred into
122 expression host *E. coli* BL21 Star (DE3). The expression of the *luxI* homologue was examined
123 *via* a cross-streak assay on the transformed host with a CV026 biosensor. AHLs produced were
124 then identified on an LC-MS/MS platform as described previously (20).
125
126 **Construction of *halI* and *halR* replacement knockout mutants**
127
128 Replacement knockout of QS genes in *H. alvei* FB1 was carried out according to Court Lab's
129 protocol "Recombineering: Using Drug Cassettes to Knock out Genes *in vivo*", downloadable
130 from the official website (https://redrecombineering.ncifcrf.gov/). Linear DNA substrates for
131 recombineering were constructed through PCR amplification with 70-base hybrid primers
132 (Table 2) consisting of 50 bases of homologous sequence that flanked the sequence to be
133 replaced and 20 bases at the 3' end that primed the amplification of the kanamycin resistance
134 (KanR) cassette from the template strain (TKC) (27). The substrates were later introduced into
135 heat-induced *H. alvei* FB1 cells harbouring pSIM7 *via* electroporation, in which the
136 recombinases were actively expressed. The recovered cells were then plated on a kanamycin
137 plate (35 µg/mL) to select for mutants that carried the KanR cassette in the place of QS genes.
138 The results of recombineering were then confirmed by colony PCR using primers (*halI*_u-F,

139 *halI*_d-R, *halR*_u-F, and *halR*_d-R with Screen_KanR-F and Screen_KanR-R, as described in
140 Table 2) that amplified the junctions where recombination took place. Cross-streaking with
141 CV026 was also performed on the *H. alvei* FB1Δ*halI*::KanR to confirm that the AHL synthase
142 function had been successfully removed.
143
144 **RNA-Seq**
145
146 *H. alvei* FB1 WT and mutant cells were grown in 200 mL LB broth at 30°C with shaking at 220
147 rpm. Readings of optical density (OD_{600}) were taken every hour. The total RNA was stabilised
148 immediately using Qiagen RNAprotect bacterial reagent (Qiagen, USA) when the cells were
149 harvested at the desired OD_{600} (0.5 and 1.5), following the manufacturer's protocol. Total
150 bacterial RNA was purified using the Qiagen RNeasy kit (Qiagen, USA) following the
151 manufacturer's protocol. Purified RNA samples were eluted in 100 µL sterile RNase-free
152 water. Total RNA from three biological replicates was obtained from independent cultures to
153 evaluate the reproducibility of RNA-Seq data. Purity of RNA samples was assessed using a
154 Nanodrop spectrophotometer (Thermo Scientific, USA), and RNA quantification was carried
155 out using the Qubit® RNA HS Assay Kit (Invitrogen, USA). The quality of the extracted RNA
156 samples was assessed with an Agilent RNA 6000 Nano Kit (Agilent Technologies, USA) using a
157 2100 Bioanalyzer.
158
159 RNA samples with RNA Integrity Number (RIN) >7.0 were chosen to proceed to rRNA
160 depletion using Ribo-Zero™ rRNA Removal Kits (Bacteria) (Epicentre, USA) prior to cDNA
161 synthesis. The quality of the rRNA-depleted RNA was assessed with an Agilent RNA 6000 Pico
162 Chip (Agilent Technologies, USA) using a 2100 Bioanalyzer. Library preparation was
163 performed following the manufacturer's protocol using the Illumina ScriptSeq™ v2 RNA-Seq
164 Library Preparation Kit (Epicentre, USA). Quality of the RNA-Seq transcriptome library was
165 examined using Agilent 2100 High Sensitivity DNA Kit. Quantification of the library was
166 assessed using the Qubit® dsDNA HS Assay Kit (Life Technologies, USA) and qPCR (KAPA
167 Biosystems) before being subjected to normalisation. The normalised samples (4 nM) were
168 denatured with 0.2 N NaOH and diluted 20 pM using pre-chilled Hybridisation Buffer (HT1)
169 (Illumina, USA). The 20 pM transcriptome libraries were further diluted to 10 pM with pre-
170 chilled HT1 buffer prior to whole transcriptome sequencing on a MiSeq platform.
171
172 RNA-seq read quality assessment was carried out using FastQC (version 0.11.2) (28).
173 Rockhopper (29, 30) was used to align the paired end reads against the *H. alvei* FB1 reference
174 genome (GenBank accession number CP009706). Differential expression analysis was then
175 performed with the DESeq2 package using the raw counts generated from Rockhopper as
176 inputs (p_{adjust} value/$q < 0.01$) (31). Gene Ontology (GO) and pathway enrichment analyses of
177 differentially expressed genes (DEGs) were performed using The Database for Annotation,
178 Visualization and Integrated Discovery (DAVID) v6.8 (32, 33)
179
180 **qPCR**
181
182 Prior to qPCR, total RNA was converted to cDNA using the QuantiTect® Reverse Transcription
183 Kit (Qiagen, Germany) following manufacturer's protocol. qPCR was performed with a CFX96
184 Touch™ Real-Time PCR Detection System (Bio-Rad, USA) using the primers listed in Table 2.

185 Expression levels in ΔΔCq of each gene were determined from analyses using Bio-Rad CFX
186 Manager version 3.1 (Bio-Rad, USA).
187
188 **Results**
189
190 **Identification of QS genes of *H. alvei***
191
192 The genome sequence of *H. alvei* FB1 is deposited in GenBank under the accession number
193 CP009706. A homology search using LuxI and LuxR amino acid sequences via the 'BLAST
194 search' function on the RAST server revealed the presence of a pair of open reading frames
195 (ORF) at position 2,668,370 – 2,669,738 in the genome that contained the signature
196 conserved domains of LuxI and LuxR homologues. The pair consisted of a 648-bp *halI* (Locus
197 tag AT03_RS12360) along with a 741-bp *halR* (AT03_RS12355). The pair was in convergent
198 orientation, with a 20-bp overlap at the 3'-ends (Figure 1A).
199
200 Multiple sequence alignment (MSA) was performed between HalI amino acid sequence and
201 other known homologues of LuxI (Figure 1B). Ten conserved key amino acid residues, namely
202 R25, F29, W35, E44, D46, D49, R70, F84, E101 and R104 according to their positions in TraI as
203 reported by Fuqua and Greenberg (34), were identified in the sequence of HalI. Likewise, MSA
204 on HalR and other known homologues of LuxR revealed the presence of six conserved key
205 residues (W57, Y61, D70, P71, W85 and G113 according to their positions in TraR) within the
206 autoinducer binding domain and three (E178, L182, and G188) within the DNA binding
207 domain (Figure 1C), as reported by Subramoni et al. (35).
208
209 Phylogenetic trees were built to illustrate the phylogenetic relationships between the HalI
210 and HalR proteins and other LuxI and LuxR homologues of known functions (Figures 1, 2).
211 Both trees shared roughly similar topologies, consisting of two major clusters. The top clusters
212 consisted solely of members of γ-Proteobacteria, whereas the bottom ones contain those of
213 α-, β- and γ-Proteobacteria. All sequences from *Hafnia* spp. formed a single clade in both
214 trees, except for an orphan LuxI homologue (YspR) in *H. paralvei* bta3-1 that clustered with
215 the more distantly related SmaR of *Serratia* sp. ATCC 39006. Both HalI and HalR were more
216 closely related to YspI-YspR in *Yersinia pestis* and YtbI-YtbR in *Y. pseudotuberculosis*,
217 compared with *Edwardsiella tarda* ATCC 15947^{T} that also belongs to the *Hafniaceae*. The LuxR
218 tree clearly shows that all the HalR sequences formed a monophyletic clade with the
219 sequences of LuxR homologues that are known to establish quorum-hindered activities.
220
221 **Expression of *halI* in a Foreign Host**
222
223 To prove the functionality of the identified AHL synthase, the *halI* sequence was cloned into
224 a pGS-21a vector and expressed in host *E. coli* BL21 Star (DE3). Cross-streaking of the
225 transformed BL21 Star (DE3) induced purple pigmentation of the CV026 biosensor (Figure S1).
226 The same AHL profile produced by *H. alvei* FB1 ($3OC_6$-HSL and $3OC_8$-HSL) was detected using
227 LC-MS/MS (Figure S2).
228
229 **Mutant Construction *via* λ-Red Recombineering**
230

231 Two mutants, namely, Δ*halI*::kanR and Δ*halR*::kanR were constructed using the λ Red
232 recombineering technique. In each mutant, either *halI* or *halR* was replaced with a kanamycin
233 resistance cassette. Verification of the mutants was performed via PCR on colonies picked
234 from LBA plates containing 35 mg/mL kanamycin. The presence of amplification products
235 encompassing the junctions between the flanking regions and a stretch of the intragenic
236 region of KanR cassette indicated the success of the replacement knockout. The PCR products
237 were sent for Sanger sequencing to confirm the sequences (Figure S3). The Δ*halI*::kanR
238 mutants, when tested by cross-streaking with biosensor CV026, were unable to induce purple
239 pigment production (Figure S4).
240
241 **RNA-Seq**
242
243 To examine the pattern of global gene expression affected by HalR regulon, RNA-Seq was
244 performed for the two mutants using strain FB1 WT as a control. Transcriptomes of each
245 strain were acquired at early- and mid-exponential phase (OD_{600} = 0.5 and 1.5, respectively).
246 Three libraries of FB1 WT, Δ*halI*::KanR, and Δ*halR*::KanR were generated for each growth
247 phase, which yielded total reads ranging from 2,124,060 to 4,957,038. The Rockhopper
248 software was able to map between 504,685 and 3,344,049 reads to the reference genome.
249 The sequencing output, along with the raw counts, have been deposited in the Gene
250 Expression Omnibus (GEO) database (https://www.ncbi.nlm.nih.gov/gds) under accession
251 number GSE93000.
252
253 **Quality Assessment of the Replicates**
254
255 The principal component analysis (PCA) plot based on the raw counts showed that, for the
256 samples harvested at OD_{600} 0.5, the three replicates of Δ*halR*::KanR samples were clearly
257 separated from the WT and Δ*halI*::KanR samples along the PC1 axis, which contributed
258 94.662% of the variation, while the latter two clustered close to each other on this axis (Figure
259 3A). For the samples harvested at OD_{600} 1.5, the replicates formed distinct clusters in different
260 quadrants of the plot, with the Δ*halI*::KanR mutant forming a cluster more distinct from the
261 WT samples along the PC1 axis (which explained 79.838% of variation) than the Δ*halR*::KanR
262 samples (Figure 3B).
263
264 **Transcriptomic Analysis of QS Mutants**
265
266 No significant differential expression ($\log_2$ fold change [FC] > 1 or < -1) was observed in the
267 Δ*halI*::KanR mutant at a *q*-value of 0.01, aside from *halI*. A total of 687 genes were found to
268 be differentially expressed in the Δ*halR*::KanR mutant, of which 511 were up-regulated
269 while 176 were down-regulated. The distribution of DEGs is illustrated as MA plots in Figure
270 4A, B.
271
272 A total of 825 and 740 genes were differentially expressed in the Δ*halI*::KanR and Δ*halR*::KanR
273 mutants, respectively. In the former, 392 were up-regulated while 433 were down-regulated,
274 while in the latter, 371 showed positive fold-changes against the WT strain while 369 showed
275 negative. The distribution of DEGs is illustrated as MA plots in Figure 4C, D, and the
276 overlapping genes between both mutants are shown in Venn diagrams (Figure 5)
277 FC of genes in each experimental condition are listed in Table S1.

For the Δ*halR*::Kan mutant in exponential phase, both up- and down-regulated gene lists were topped by genes involved in carbohydrate transport and metabolism. Up-regulated genes were mainly involved with ribose metabolism, whereas down-regulated genes involved in mannitol, maltose and galactose uptake were among those with the highest FCs. In mid-exponential phase, genes involved in amino acid transport and metabolism were most abundant in the lists of both mutants. Genes involved with maltose transport, for instance maltoporin, which were down-regulated in the early exponential phase, were up-regulated in the mid-exponential phase.

GO and Pathway Enrichment Analysis of QS-dependent Genes

GO enrichment analysis was performed on the DEGs to gain an insight into the QS-regulated genes. At the early exponential phase, out of the 511 up-regulated genes in the Δ*halR*::KanR mutant, 438 were assigned to 197 GO terms, of which five terms were enriched (q-value < 0.01). Of the 176 down-regulated genes, 114 were assigned to 58 terms, of which only two were enriched (Figure 6). The GO terms enriched in the up-regulated DEGs included fatty acid biosynthetic processes, cytoplasm, ATP binding, RNA binding, and tRNA binding, whereas the down-regulated genes included those involved in the phosphoenolpyruvate-dependent sugar phosphotransferase system and in response to stress.

In the mid-exponential phase, 304 out of 371 up-regulated genes in the Δ*halR*::KanR mutant were assigned to 180 GO terms, and two (phosphoenolpyruvate-dependent sugar phosphotransferase system and cobalamin biosynthesis process) were significantly enriched. Of the 263 GO terms accounting for 317 of the 369 down-regulated genes, only one (TCA cycle) was significantly enriched. In the *halI* mutant, genes with positive and negative FCs were assigned to 132 and 138 GO terms, respectively. None of these terms were enriched at q-value = 0.01.

DEGs were also mapped into the KEGG pathway database to identify pathways that were significantly enriched in each experimental condition (Figure 10). In early exponential phase, the up-regulated genes in the Δ*halR*::KanR mutant were assigned to a total of 80 pathways, of which 12 were significantly enriched at the cut-off of q-value = 0.01. These pathways included primarily those involved in biosynthesis of molecules and functions that involved nucleotides. Six of the 59 pathways to which the down-regulated genes in the Δ*halR*::KanR mutant were assigned were significantly enriched. As in the GO ontology, the phosphotransferase system (PTS) was involved, along with several other pathways involved in carbohydrate metabolism.

In mid-exponential phase, the number of down-regulated pathways in the Δ*halR*::KanR mutant far exceeded those that were up-regulated. A total of 30 out of 80 pathways were significantly enriched. These pathways were mostly involved in amino acid metabolism. The Δ*halI*::KanR mutant in the same growth phase showed a much smaller number of enriched pathways than did the Δ*halR*::KanR, but they were still dominated by down-regulated genes. Most of these pathways overlapped those affected in the *halR* counterpart, except for beta-lactam resistance.

Validation of RNA-Seq Data by qPCR

To validate the RNA-Seq results, six genes were randomly chosen for qPCR. The $\log_2$ FCs of qPCR were calculated and plotted against that of RNA-Seq (Figure 8). The correlation coefficients were all above 0.99, indicating that the results obtained were reliable

Discussion

Having examined *in silico* the characteristics of the candidates of QS genes in *H. alvei* FB1, the strain, unlike some other members of Proteobacteria, possessed only a single pair of *luxI-luxR* homologues. The presence of conserved domains and amino acid sites that are signature to the group of proteins, along with the orientation of the genes, provide strong evidence supporting the identity of the QS gene candidates. Phylogenetic trees constructed using choices of sequences included in the analyses adapted from a review by Tsai and Winans (36) revealed that the amino acid sequences of HalR proteins obtained from members of the genus *Hafnia* fell into a monophyletic clade with other EsaR-like proteins. This, along with other traits, such as a convergent orientation with overlapping 3'-ends and responding to $3OC_6$-HSL, suggested the possibility that HalR might establish similar quorum-hindered behaviour. An intermingling pattern between sequences originating from genomes that belonged to different classes of Proteobacteria was observed in one of the major clusters in both phylogenetic trees. This observation, along with the distant phylogenetic relationship between the orphan LuxR homologue with HalR, is likely to reflect the occurrence of HGT in the past, as has been reported in previous studies (37, 38).

According to the results of the transcriptomic study, Δ*halI*::KanR and Δ*halR*::KanR mutants showed difference in the functional distribution patterns of DEGs, which supports the proposition that HalR proteins belong to the quorum-hindered group. At early exponential phase, no significant DEG was observed in Δ*halI*::KanR, whereas a large number of DEGs were found in Δ*halR*::KanR. We suggest that, at OD_{600} of 0.5, the concentration of AHLs within the culture environment was still too low to affect the expression of any genes. Therefore, the mutant lacking AHL-synthase established a gene expression profile similar to the WT strain. The observation that removal of the *halR* gene resulted in a very different expression profile pointed to the possibility that there were HalR proteins already binding at the promoter regions of certain genes at this early stage, playing a regulatory role in the absence of sufficient QS signals. A much larger number of up-regulated genes was observed in the Δ*halR*::KanR mutant compared with those that were down-regulated, indicating that the major role of the HalR protein at this stage could be repression of certain functions in an early growth phase.

Later, in the mid-exponential phase, the gene expression profiles in the two mutants changed. As illustrated by PCA, the Δ*halR*::KanR mutant now clustered closer to the WT strain, implying that, with the increasing concentration of AHL molecules over time, the HalR proteins in FB1 WT were then released from their binding sites and the expression levels of the previously repressed genes became similar to the unrepressed ones in Δ*halR*::KanR. At this stage, DEGs could also be observed in the Δ*halI*::KanR mutant. More than half of these genes showed changes in the same directions in both mutants, which reflected a scenario more complex than classical examples of 'quorum-hindered apo-proteins', in which the changes in both

371 mutants were expected to be in opposite directions. This observation suggests that a more
372 complicated regulatory mechanism could be involved in the QS system in *H. alvei*.
373
374 **Functional Distribution of QS-regulated Genes**
375
376 The enrichment analyses revealed that, in the early exponential phase, a number of traits
377 related to dormancy and survival under stressful conditions were affected by the removal of
378 the *halR* gene. The four GO terms most significantly enriched for up-regulated genes in the
379 exponential phase (cytoplasm, RNA binding, ATP binding, and tRNA binding) contained DEGs
380 that could be generalised into three categories: DNA replication (helicases, gyrase, and
381 topoisomerase), mismatch repair (*mutS*), and protein biosynthesis (rRNA and tRNA
382 methyltransferases, aminoacyl-tRNA synthetases), corresponding to the enriched KEGG
383 pathways (Aminoacyl-tRNA biosynthesis, DNA replication, Mismatch repair, and Protein
384 export)(Figure 7). Genes involved in metabolism of ribose, an important building block of DNA
385 and RNA backbones, were amongst the genes with the highest FCs. This up-regulation
386 occurring in the absence of HalR indicated that metabolism of nucleic acids was highly
387 repressed in WT cells. Fatty acid biosynthesis was also amongst the up-regulated functions in
388 both analyses, suggesting that the cell membrane biosynthesis was also repressed. Regulation
389 of chromosomal replication and cell division by QS has been reported in *E. coli* (39, 40) and *P.*
390 *aeruginosa* (41).
391
392 Genes involved in stress response and sugar uptake were negatively affected in the
393 Δ*halR*::KanR mutant, which could be reflected in the down-regulation of two biological
394 process terms (stress response and phosphoenolpyruvate-dependent sugar
395 phosphotransferase system) and five pathways (phosphotransferase systems, carbon
396 metabolism, microbial metabolism in diverse environments, fructose and mannose
397 metabolism, and citrate cycle). Several genes involved in PTS with specificity towards
398 mannitol and ascorbate, along with a number of other sugar permeases and transporters,
399 such as maltose, fructose, and galactose, were amongst the genes with significant FC.
400
401 In the mid-exponential phase, the expression profile in the Δ*halR*::KanR mutant changed
402 drastically. At this stage, many pathways involved in amino acid and fatty acid metabolism
403 were down-regulated. In other words, these pathways were expressed at a higher level in the
404 WT strain compared with the mutants, indicating that quorum sensing played a significant
405 role in promoting metabolic activities in *H. alvei* FB1. The results of the GO enrichment
406 analysis implied that phosphotransferase systems that were activated in WT earlier were now
407 repressed, suggesting that these functions were more important in the early than in the mid-
408 exponential phase. PTS are known to work not only as carbohydrate transport and
409 modification systems in all phyla of bacteria, but also have regulatory roles in numerous
410 cellular functions (42). In *E. coli*, glucose-specific PTS was found to inhibit other non-PTS sugar
411 permeases influencing the availability of glucose *via* dephosphorylation of the EIIA subunit
412 (43). This phenomenon, termed "catabolite repression", contributes to the establishment of
413 a hierarchy of sugar utilisation, which allows bacteria to utilise energy sources in an
414 economical manner, as well as a regulatory circuit that acts according to nutrient availability
415 (44).
416

The overall picture gained from these observations is that QS appears to be involved in repressing the functions involved in cell growth in an early growth phase, where the cells are still in the process of recovery from stationary phase stress, in a typical 'quorum-hindered apo-protein' manner. The repressed genes may then be re-activated at a later stage when the DNA-bound apo-proteins are 'hindered' by the presence of AHL molecules at high cell density. Apo-HalR, on the other hand, could positively regulate the stress response and sugar uptake functions in the early exponential phase. PTS and various sugar transport systems that are active at low cell density could provide a mechanism for detection of nutrient availability and management of energy consumption. Whether these events of repression and activation are interdependent or under separate regulatory control will require further studies to resolve.

The observation that both mutants shared more than half of their enriched pathways in mid-exponential phase strongly suggests that QS regulation operated in a manner different to the early exponential phase. In contrast with the expectation in a 'quorum-hindered apo-protein' model, very few DEGs showed contradicting expression levels between the two mutants at this stage. Further study is required to provide a strong basis for the understanding of the regulatory mechanism of the HalR protein.

Author statements

Authors and contributors

JYT conceived and designed the experiments, performed the experiments, analysed the data, wrote the paper, and prepared figures and/ or tables. WSST conceived and designed the experiments, performed the experiments, and analysed the data. PC reviewed the manuscript. K-GC supervised the project, contributed reagents/ materials/analysis tools. All authors approved the manuscript.

Conflicts of interest

The authors declare that there are no conflicts of interest.

Acknowledgements

K-GC thanks the research grants from the University of Malaya (FRGS grant FP022-2018A, PPP grant PG136-2016A, and HIR grant H-50001-A000027). PC is supported by NERC core funding to the British Antarctic Survey's 'Biodiversity, Evolution and Adaptation' Team.

References

Miller MB, Bassler BL. Quorum sensing in bacteria. *Annu Rev Microbiol* 2001; 55:165-199.

2. **Parsek MR, Greenberg EP.** Acyl-homoserine lactone quorum sensing in Gram-negative bacteria: a signaling mechanism involved in associations with higher organisms. *Proc Natl Acad Sci U S A* 2000; 97:8789-8793.
3. **Duerkop BA, Ulrich RL, Greenberg EP.** Octanoyl-homoserine lactone is the cognate signal for *Burkholderia mallei* BmaR1-BmaI1 quorum sensing. *J Bacteriol* 2007; 189:5034-5040.
4. **Hao G, Burr TJ.** Regulation of long-chain N-acyl-homoserine lactones in *Agrobacterium vitis*. *J Bacteriol* 2006; 188:2173-2183.
5. **Pearson JP, Feldman M, Iglewski BH, Prince A**. *Pseudomonas aeruginosa* cell-to-cell signaling is required for virulence in a model of acute pulmonary infection. I*nfect Immun* 2000; 68:4331-4334.

465 6. **Barnard AM, Bowden SD, Burr T, Coulthurst SJ, Monson RE, Salmond GP**. Quorum
466 sensing, virulence and secondary metabolite production in plant soft-rotting
467 bacteria. *Philos Trans R Soc Lond B Biol Sci* 2007; 362:1165-1183.
468 7. **Pierson LS, Gaffney T, Lam S, Gong F**. Molecular analysis of genes encoding
469 phenazine biosynthesis in the biological control bacterium, *Pseudomonas*
470 *aureofaciens* 30-84. *FEMS Microbiol Lett* 1995; 134:299-307.
471 8. **Rivas M, Seeger M, Jedlicki E, Holmes DS**. Second acyl homoserine lactone
472 production system in the extreme acidophile *Acidithiobacillus ferrooxidans*. *Appl*
473 *Environ Microbiol* 2007; 73:3225-3231.
474 9. **Tomlin KL, Malott RJ, Ramage G, Storey DG, Sokol PA, Ceri H**. Quorum-sensing
475 mutations affect attachment and stability of *Burkholderia cenocepacia* biofilms. *Appl*
476 *Environ Microbiol* 2005; 71:5208-5218.
477 10. **Labbate M, Queck SY, Koh KS, Rice SA, Givskov M, Kjelleberg S**. Quorum sensing-
478 controlled biofilm development in *Serratia liquefaciens* MG1. *J Bacteriol* 2004;
479 186:692-698.
480 11. **Blana VA, Nychas GJ.** Presence of quorum sensing signal molecules in minced beef
481 stored under various temperature and packaging conditions. *Int J Food Microbiol*
482 2014; 173:1-8.
483 12. **Bruhn JB, Christensen AB, Flodgaard LR, Nielsen KF, Larsen TO, *et al.*** Presence of
484 acylated homoserine lactones (AHLs) and AHL-producing bacteria in meat and
485 potential role of AHL in spoilage of meat. *Appl Environ Microbiol* 2004; 70:4293-
486 4302.
487 13. **Christensen AB, Riedel K, Eberl L, Flodgaard LR, Molin S, *et al*.** Quorum-sensing-
488 directed protein expression in *Serratia proteamaculans* B5a. *Microbiology* 2003;
489 149:471-483.
490 14. G**ram L, Christensen AB, Ravn L, Molin S, Givskov M.** Production of acylated
491 homoserine lactones by psychrotrophic members of the Enterobacteriaceae isolated
492 from foods. *Appl Environ Microbiol* 1999; 65:3458-3463.
493 15. **Ridell J, Korkeala H.** Minimum growth temperatures of *Hafnia alvei* and other
494 Enterobacteriaceae isolated from refrigerated meat determined with a temperature
495 gradient incubator. *Int J Food Microbiol* 1997; 35:287-292.
496 16. **Janda JM, Abbott SL.** The genus *Hafnia*: from soup to nuts. *Clin Microbiol Rev* 2006;
497 19:12-18.
498 17. **Milani C, Ticinesi A, Gerritsen J, Nouvenne A, Lugli GA, *et al.*** Gut microbiota
499 composition and *Clostridium difficile* infection in hospitalized elderly individuals: a
500 metagenomic study. *Sci Rep* 2016; 6:25945.
501 18. **Carding S, Verbeke K, Vipond DT, Corfe BM, Owen LJ.** Dysbiosis of the gut
502 microbiota in disease. *Microb Ecol Health Dis* 2015; 26:26191.
503 19. **Jiang H, Ling Z, Zhang Y, Mao H, Ma Z, *et al*.** Altered fecal microbiota composition in
504 patients with major depressive disorder. *Brain Behav Immun* 2015; 48:186-194.
505 20. **Tan JY, Yin WF, Chan KG**. Quorum sensing activity of *Hafnia alvei* isolated from
506 packed food. *Sensors (Basel)* 2014; 14:6788-6796.
507 21. **Chin CS, Alexander DH, Marks P, Klammer AA, Drake J, *et al*.** Nonhybrid, finished
508 microbial genome assemblies from long-read SMRT sequencing data. *Nat Methods*
509 2013; 10:563-569.
510 22. **Aziz RK, Bartels D, Best AA, DeJongh M, Disz T, *et al.*** The RAST Server: rapid
511 annotations using subsystems technology. *BMC Genomics* 2008; 9:75.

512 23. **Aziz RK, Devoid S, Disz T, Edwards RA, Henry CS, *et al*.** SEED servers: high-
513 performance access to the SEED genomes, annotations, and metabolic models. *PLoS*
514 *One* 2012; 7:e48053.
515 24. **Angiuoli SV, Gussman A, Klimke W, Cochrane G, Field D, *et al*.** Toward an online
516 repository of Standard Operating Procedures (SOPs) for (meta)genomic annotation.
517 *OMICS* 2008; 12:137-141.
518 25. **Marchler-Bauer A, Bo Y, Han L, He J, Lanczycki CJ, *et al*.** CDD/SPARCLE: functional
519 classification of proteins via subfamily domain architectures. *Nucleic Acids Res* 2017;
520 45:D200-D203.
521 26. **Galtier N, Gouy M, Gautier C.** SEAVIEW and PHYLO_WIN: two graphic tools for
522 sequence alignment and molecular phylogeny. *Comput Appl Biosci* 1996; 12:543-548.
523 27. **Sharan SK, Thomason LC, Kuznetsov SG, Court DL**. Recombineering: a homologous
524 recombination-based method of genetic engineering. *Nat Protoc* 2009; 4:206-223.
525 28. **Andrews S.** FastQC: a quality control tool for high throughput sequence data. 2010.
526 Available online at: http://www.bioinformatics.babraham.ac.uk/projects/fastqc
527 29. **McClure R, Tjaden B, Genco C**. dentification of sRNAs expressed by the human
528 pathogen *Neisseria gonorrhoeae* under disparate growth conditions. *Front Microbiol*
529 2014; 5:456.
530 30. **Tjaden B**. De novo assembly of bacterial transcriptomes from RNA-seq data. *Genome*
531 *Biol* 2015; 16:1.
532 31. **Love MI, Huber W, Anders S.** Moderated estimation of fold change and dispersion
533 for RNA-seq data with DESeq2. *Genome Biol* 2014; 15:550.
534 32. **Huang dW, Sherman BT, Lempicki RA.** Bioinformatics enrichment tools: paths
535 toward the comprehensive functional analysis of large gene lists. *Nucleic Acids Res*
536 2009; 37:1-13.
537 33. **Huang dW, Sherman BT, Lempicki RA**. Systematic and integrative analysis of large
538 gene lists using DAVID bioinformatics resources. *Nat Protoc* 2009; 4:44-57.
539 34. **Fuqua C, Greenberg EP.** Listening in on bacteria: acyl-homoserine lactone signalling.
540 *Nat Rev Mol Cell Biol* 2002; 3:685-695.
541 35. **Subramoni S, Florez Salcedo DV, Suarez-Moreno ZR.** A bioinformatic survey of
542 distribution, conservation, and probable functions of LuxR solo regulators in
543 bacteria. *Front Cell Infect Microbiol* 2015; 5:16.
544 36. **Tsai CS, Winans SC.** LuxR-type quorum-sensing regulators that are detached from
545 common scents. *Mol Microbiol* 2010; 77:1072-1082.
546 37. **Hao Y, Winans SC, Glick BR, Charles TC.** Identification and characterization of new
547 LuxR/LuxI-type quorum sensing systems from metagenomic libraries. *Environ*
548 *Microbiol* 2010; 12:105-117.
549 38. **Gray KM, Garey JR**. The evolution of bacterial LuxI and LuxR quorum sensing
550 regulators. *Microbiology* 2001; 147:2379-2387.
551 39. **DeLisa MP, Wu CF, Wang L, Valdes JJ, Bentley WE.** DNA microarray-based
552 identification of genes controlled by autoinducer 2-stimulated quorum sensing in
553 *Escherichia coli. J Bacteriol* 2001; 183:5239-5247.
554 40. **Withers HL, Nordström K.** Quorum-sensing acts at initiation of chromosomal
555 replication in *Escherichia coli*. *Proc Natl Acad Sci U S A* 1998; 95:15694-15699.
556 41. **Wagner VE, Bushnell D, Passador L, Brooks AI, Iglewski BH.** Microarray analysis of
557 *Pseudomonas aeruginosa* quorum-sensing regulons: effects of growth phase and
558 environment. *J Bacteriol* 2003; 185:2080-2095.

42. **Galinier A, Deutscher J.** Sophisticated regulation of transcriptional factors by the bacterial phosphoenolpyruvate: sugar phosphotransferase system. *J Mol Biol* 2017; 429:773-789.
43. **Kotrba P, Inui M, Yukawa H.** Bacterial phosphotransferase system (PTS) in carbohydrate uptake and control of carbon metabolism. *J Biosci Bioeng* 2001; 92:502-517.
44. **Brückner R, Titgemeyer F.** Carbon catabolite repression in bacteria: choice of the carbon source and autoregulatory limitation of sugar utilization. *FEMS Microbiol Lett* 2002; 209:141-148.

598 **Table 1: Bacterial strains and plasmids used in this study**

Strains or plasmids	Description	Genotype	Source/Reference
Chromobacterium violaceum CV026	Biosensor that produce purple coloured pigment (violacein) in the presence of short chain AHLs	*cviI*::mini-Tn*5*	(McClean et al., 1997)
E. coli DH5α	Laboratory strain engineered to maximise transformation efficiency; host to pSIM7	F^- Φ80*lac*ZΔM15 Δ(*lac*ZYA-*arg*F) U169 *rec*A1 *end*A1 *hsd*R17 (rK^-, mK^+) *pho*A *sup*E44 λ– *thi*-1 *gyr*A96 *rel*A1	Invitrogen, USA
E. coli TKC	Laboratory strain engineered to carry multiple drug cassette that served as templates for recombineering substrates.	*tetA, cat, kan*	Court Lab (court@ncifcrf.gov)
Hafnia alvei FB1	Isolate from fish ball	WT	This study
Hafnia alvei FB1-Δ*halI*::*kan*	Mutant with AHL synthase gene replaced by a kanamycin resistance cassette	Δ*halI*::*kan*	This study
Hafnia alvei FB1-Δ*halR*::*kan*	Mutant with AHL receptor gene replaced by a kanamycin resistance cassette	Δ*halR*::*kan*	This study
pSIM7	pBBR1 expressing the λ-Red 'recombinase' genes	Gam, Exo, and Bet; Chloramphenicol resistance	Court Lab (court@ncifcrf.gov)

599

600

601

602 **Table 2:** Oligonucleotides used in PCR amplification for mutant construction.

Primers	**Sequence (5' – 3')**	**Annealing temperature (°C)**	**Length (-mer)**	**Reference**
halI-KanR-F	ATA GCA GGA CGC GAA AAA CAC CAG CCA TAG ATA ATA TGG ATA GTA ACT AAA ATG TAA TCA AGG TGA TGG ATA TGG ACA GCA AGC GAA CCG	72	90	This study
halI-KanR-R	AGT AAG CAA CGC CCG ACA AGC AAT AAG GTT GGG CGT TGA ACT TGA TCT TAT TAC ACC AAT GCA GGC GTA ATC AGA AGA ACT CGT CAA GAA G		91	This study
halR-KanR-F	GTA CTT TGC GCC CTG TAC TTA AGT GCA TGT TGT CAC TCA GAC ATG GGA AAT TGA ACG TCT AGG AGC CCA ATA TGG ACA GCA AGC GAA CCG	72	90	This study
halR-KanR-R	AGT CGG TGG TAT TCA GTC CCA GAT GGT TAA TTG GCC AAT GTC GAT AGC CGT TAC GCC TGC ATT GGT GTA ATC AGA AGA ACT CGT CAA GAA G		91	This study
*halI*_u-F	CCA GCC ATA GAT AAT ATG GA	50 (with Screen_KanR-R)	20	This study
*halI*_d-R	AGT AAG CAA CGC CCG ACA AG	50 (with Screen_KanR-F)	20	This study
*halR*_u-F	AAG TGC ATG TTG TCA CTC AG	50 (with Screen_KanR-R)	20	This study
*halR*_d-R	AGT CGG TGG TAT TCA GTC CC	50 (with Screen_KanR-F)	20	This study
Screen_KanR-F	CAC TGA GTT TCA CGA GGA CT		20	This study
Screen_KanR-R	TGA ACG CAC CGT TAA ATT CC		20	This study

603

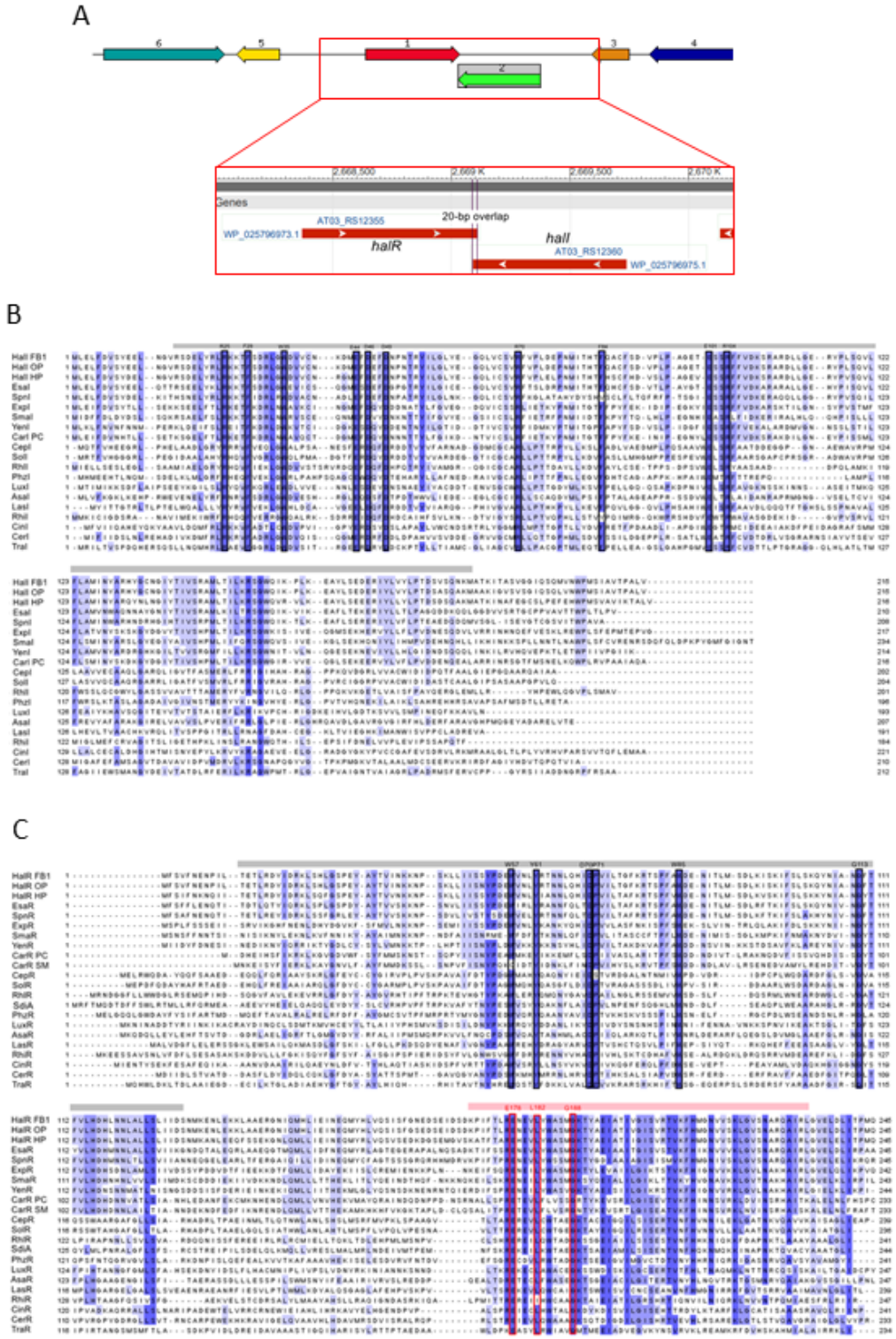

Figure 1: Physical map and sequence analyses of HalI and HalR in *H. alvei* FB1. (A) The arrows indicate the coding regions of *halI* and *halR*, along with the orientation and the flanking genes. 1. *halR*; 2. *halI*; 3. Hypothetical protein; 4. Probable secreted protein; 5. Permease of the drug/metabolite transporter (DMT) superfamily; 6. *umuC*. (B) MSA of amino acid sequences of HalI and other known LuxI homologues. Ten key conserved residues according to their positions in TraI are highlighted. OP: *O. proteus*; HP: *H. paralvei*; PC: *P. carotovorum*. (C) MSA of amino acid sequences of HalR and other known LuxR homologues. Nine key conserved residues within DNA binding domain according to their positions in TraR are highlighted. OP: *O. proteus*; HP: *H. paralvei*; PC: *P. carotovorum*.

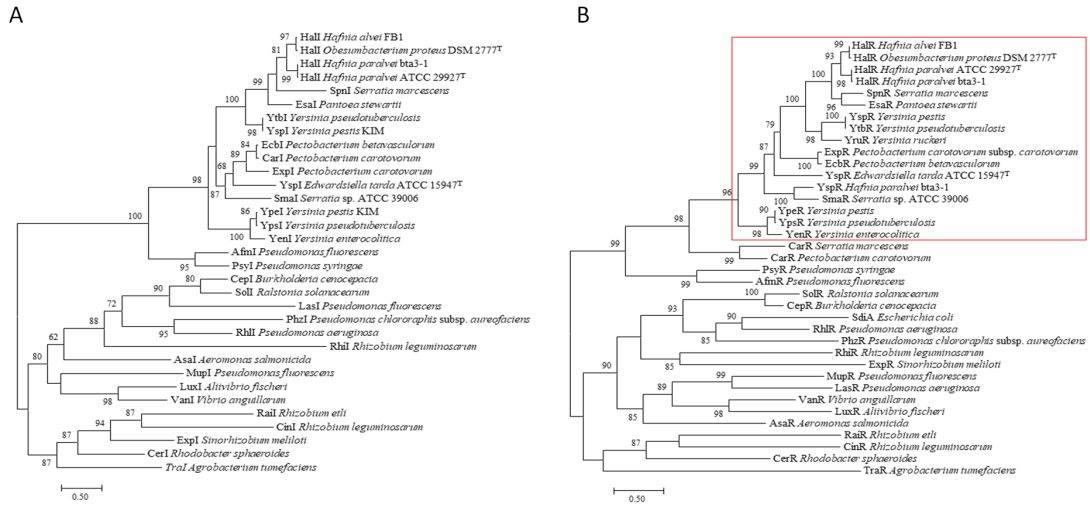

Figure 2: (A) Phylogenetic tree showing the evolutionary distance of HalI of *H. alvei* FB1 and other LuxI homologues inferred using the Maximum Likelihood (PhyML) method based on the LG matrix-based model. The tree with the highest log likelihood (-11301.6) is shown. The aLRT branch support values are shown next to the branches. The tree is drawn to scale, with branch lengths measured in 0.5 substitutions per site (bar). (B) Phylogenetic tree showing the evolutionary distance of HalR of *H. alvei* FB1 and other LuxR homologues inferred using the Maximum Likelihood (PhyML) method based on the LG matrix-based model. The tree with the highest log likelihood (-14799.2) is shown. The aLRT branch support values are shown next to the branches. The tree is drawn to scale, with branch lengths measured in 0.5 substitutions per site (bar). The monophyletic clade that contained HalR and other LuxR homologues known to establish quorum-hindered properties is highlighted in the red box.

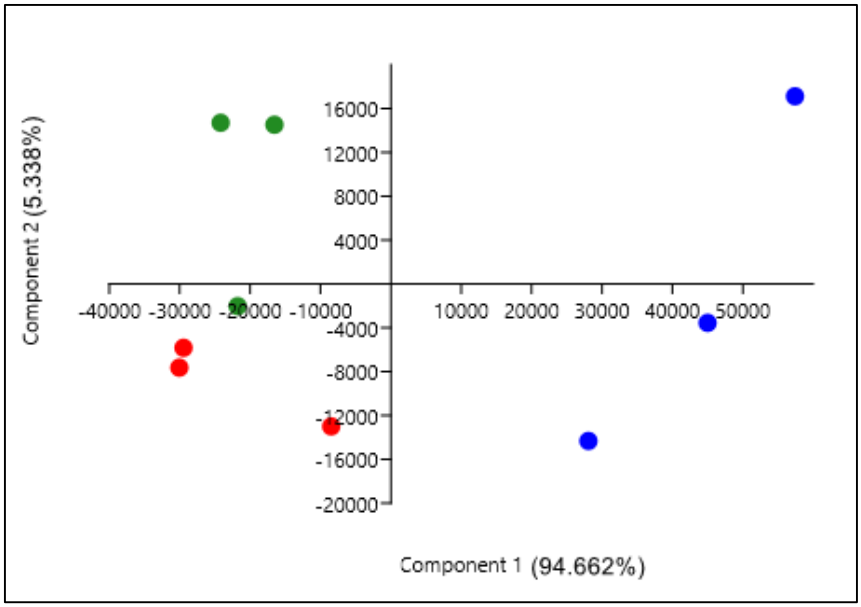

(A)

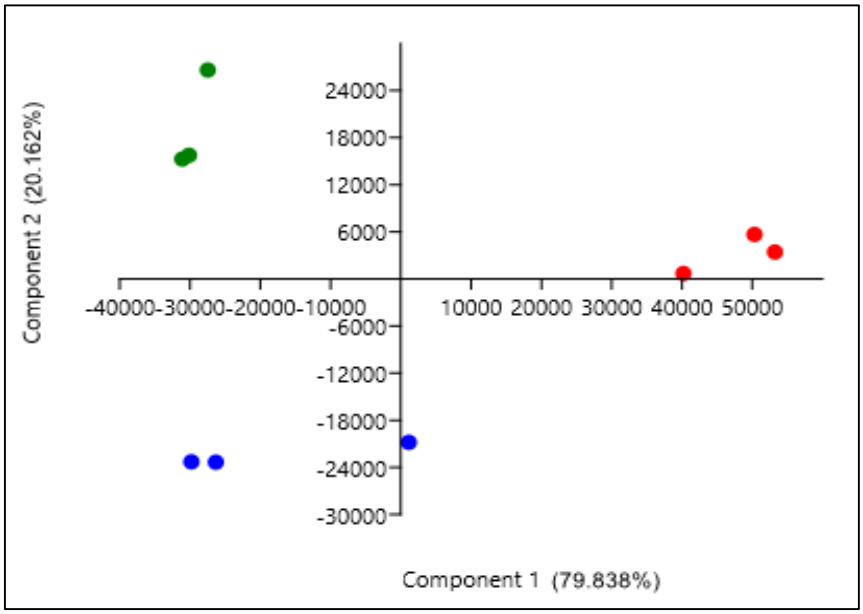

(B)

Figure 3: PCA scatter plots showing the variation between samples and consistency between replicates. Triplicates of *H. alvei* FB1 WT, Δ*halI*::KanR, and Δ*halR*::KanR are represented as green, red, and blue dots, respectively. (A) Samples harvested in early exponential phase. (B) Samples harvested in mid-exponential phase.

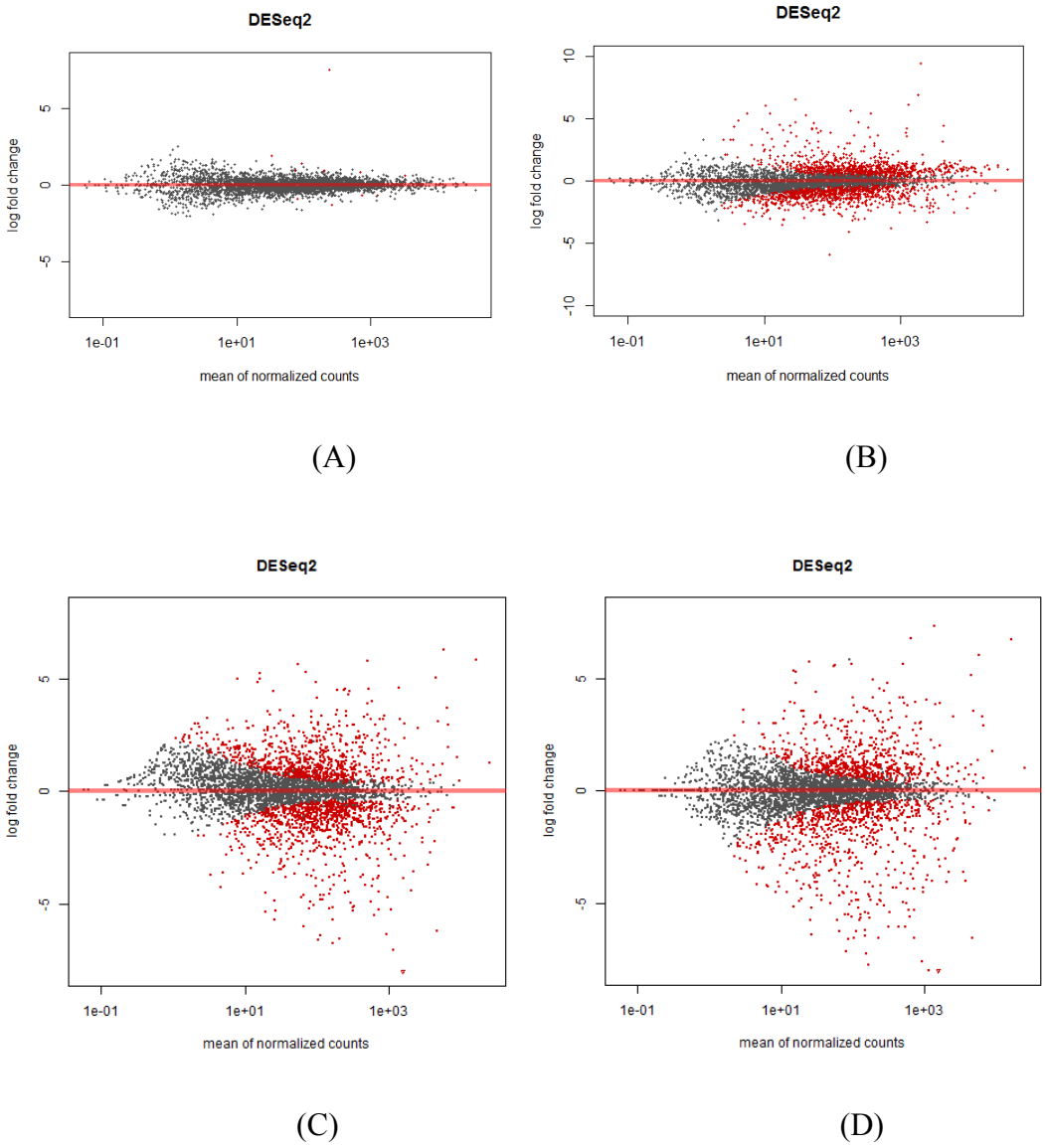

Figure 4: MA plots showing the distribution of DEGs in (A) Δ*halI*::KanR and (B) Δ*halR*::KanR against WT in early exponential phase and (C) Δ*halI*::KanR and (D) Δ*halR*::KanR against WT in mid-exponential phase. Grey dots: genes with $\log_2$ FCs below 1 and above -1; red dots: genes with $\log_2$ FCs above 1 and below -1.

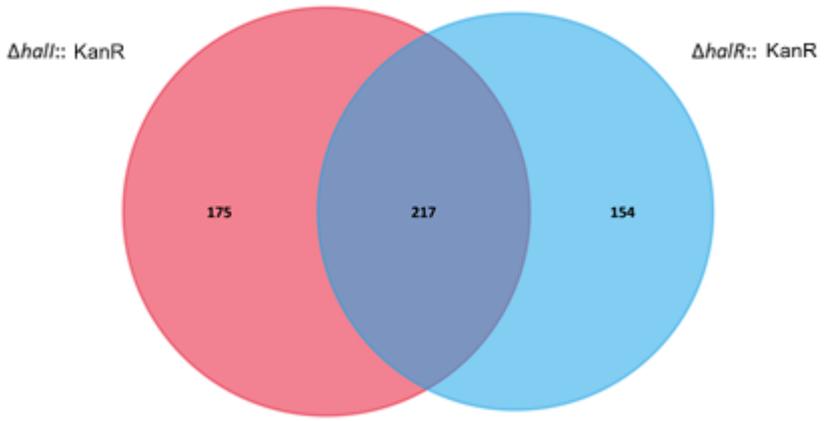

(A)

(B)

Figure 5: Venn diagrams showing the overlapping DEGs between Δ*halI*::KanR and Δ*halR*::KanR mutants in mid-exponential phase. (A) A total of 217 up-regulated genes ($\log_2$ FC > 1, *q*-value < 0.01) are shared between Δ*halI*::KanR (red circle) and Δ*halR*::KanR (blue circle), which contain 175 and 154 unique up-regulated genes, respectively, (B) A total of 273 down-regulated genes ($\log_2$ FC < -1, *q*-value < 0.01) are shared between Δ*halI*::KanR (red circle) and Δ*halR*::KanR (blue circle), which contain 160 and 96 unique down-regulated genes, respectively.

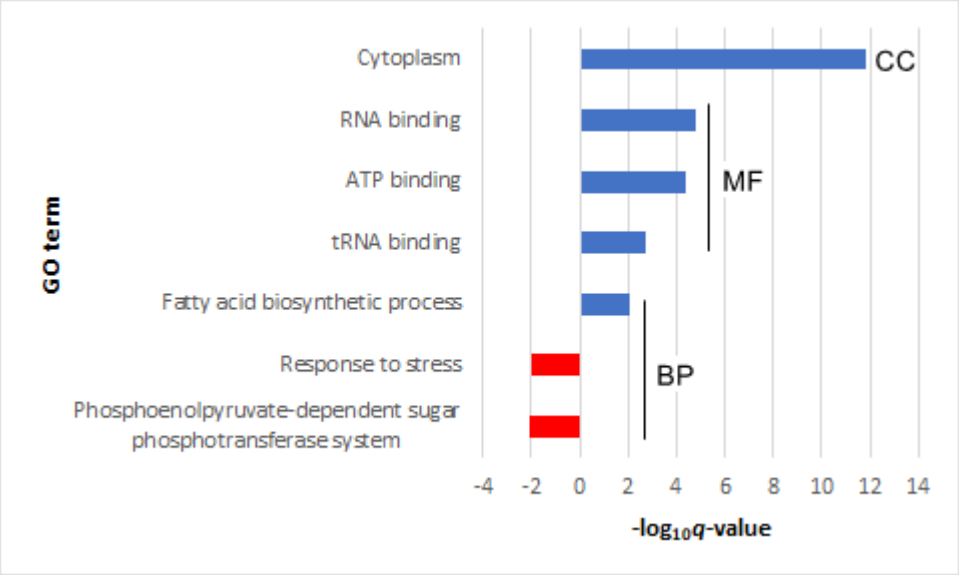

(A)

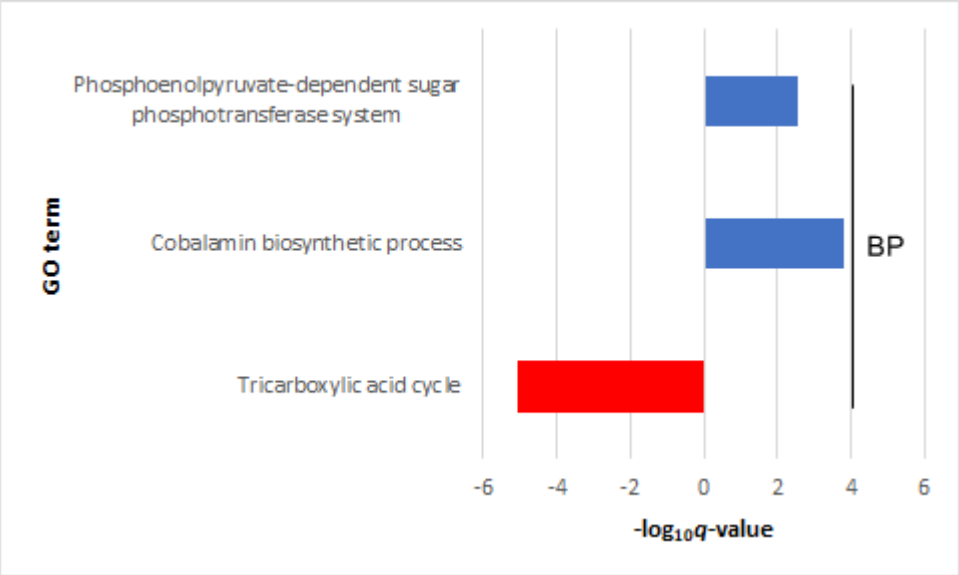

(B)

Figure 6: GO enrichment grouping of QS-dependent genes in *halR*::KanR in (A) early exponential phase and (B) mid-exponential phase. CC: Cellular content; MF: Molecular function; BP: Biological process.

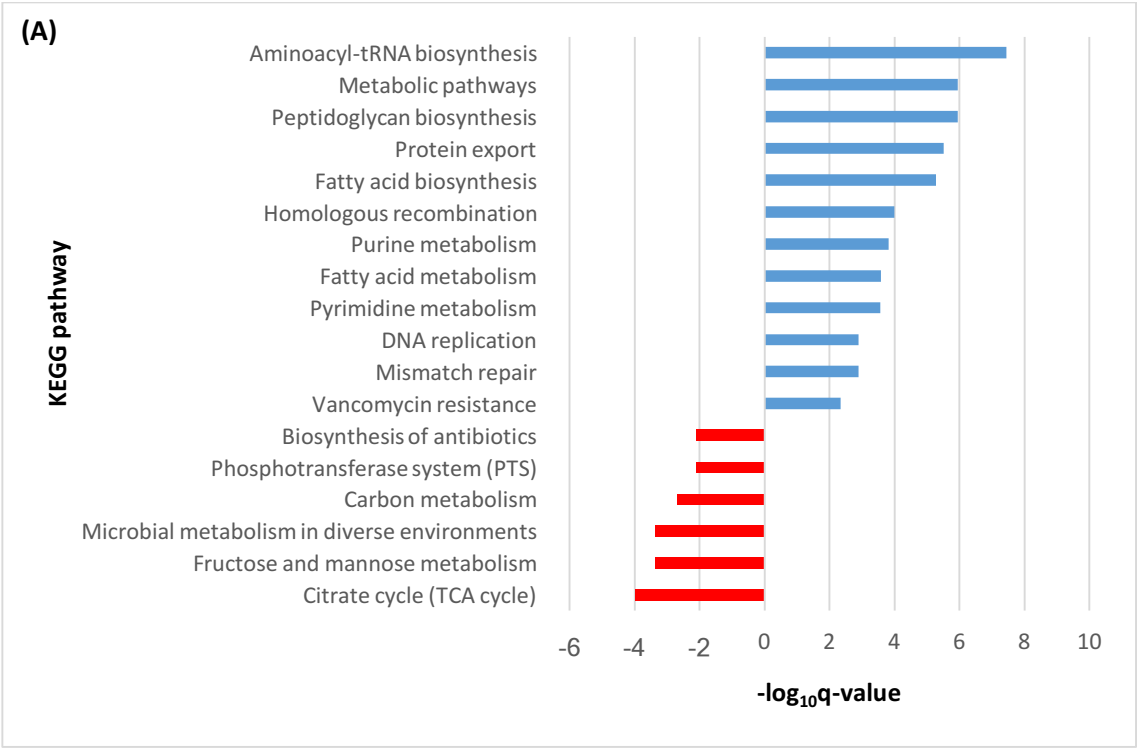
(A)
KEGG pathway
Aminoacyl-tRNA biosynthesis
Metabolic pathways
Peptidoglycan biosynthesis
Protein export
Fatty acid biosynthesis
Homologous recombination
Purine metabolism
Fatty acid metabolism
Pyrimidine metabolism
DNA replication
Mismatch repair
Vancomycin resistance
Biosynthesis of antibiotics
Phosphotransferase system (PTS)
Carbon metabolism
Microbial metabolism in diverse environments
Fructose and mannose metabolism
Citrate cycle (TCA cycle)
-6
-4
-2
0
2
4
6
8
10
-log10q-value

661

(B)

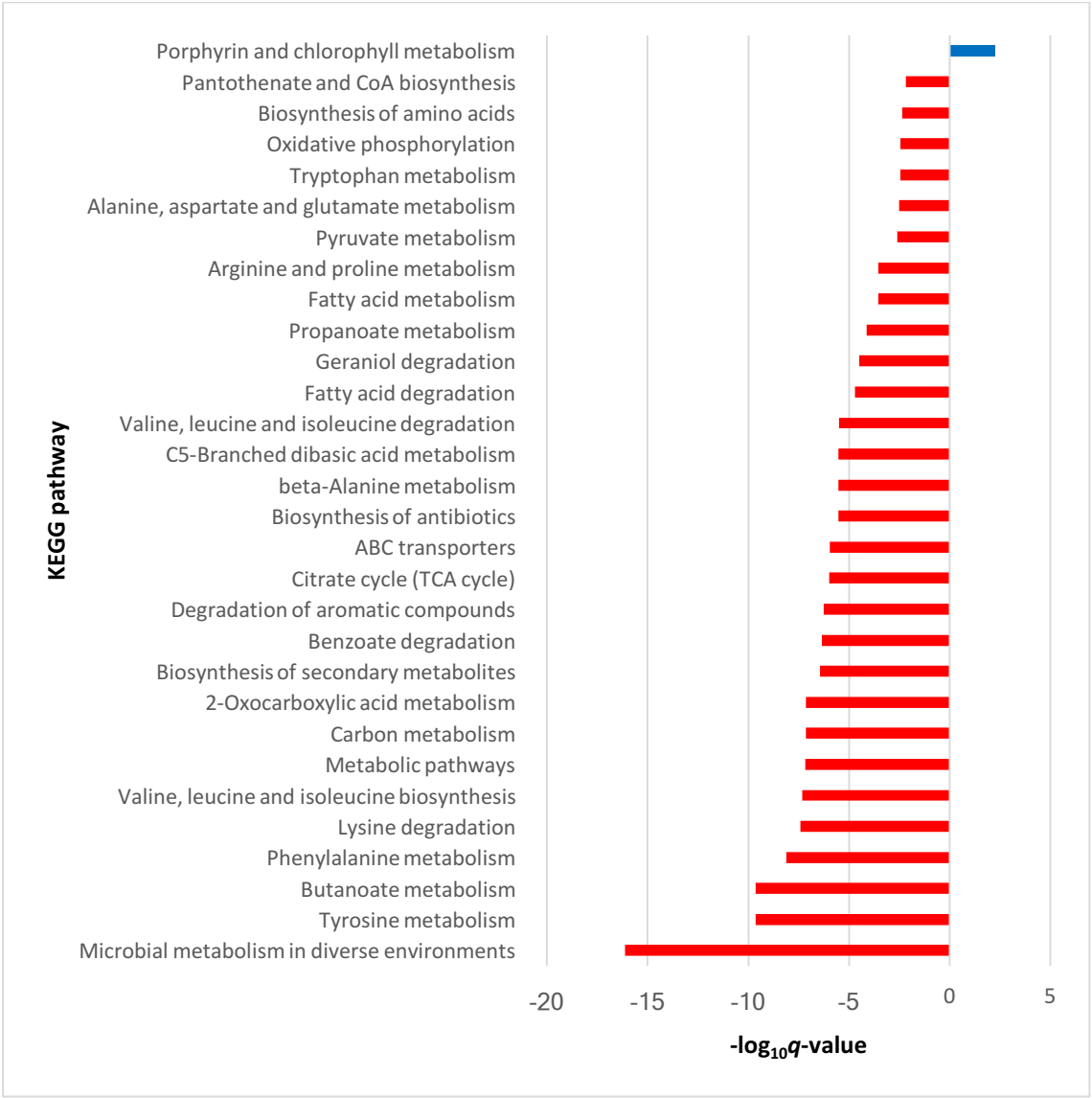
Porphyrin and chlorophyll metabolism
Pantothenate and CoA biosynthesis
Biosynthesis of amino acids
Oxidative phosphorylation
Tryptophan metabolism
Alanine, aspartate and glutamate metabolism
Pyruvate metabolism
Arginine and proline metabolism
Fatty acid metabolism
Propanoate metabolism
Geraniol degradation
Fatty acid degradation
Valine, leucine and isoleucine degradation
C5-Branched dibasic acid metabolism
beta-Alanine metabolism
Biosynthesis of antibiotics
ABC transporters
Citrate cycle (TCA cycle)
Degradation of aromatic compounds
Benzoate degradation
Biosynthesis of secondary metabolites
2-Oxocarboxylic acid metabolism
Carbon metabolism
Metabolic pathways
Valine, leucine and isoleucine biosynthesis
Lysine degradation
Phenylalanine metabolism
Butanoate metabolism
Tyrosine metabolism
Microbial metabolism in diverse environments
KEGG pathway
-20
-15
-10
-5
0
5
-log10q-value

662

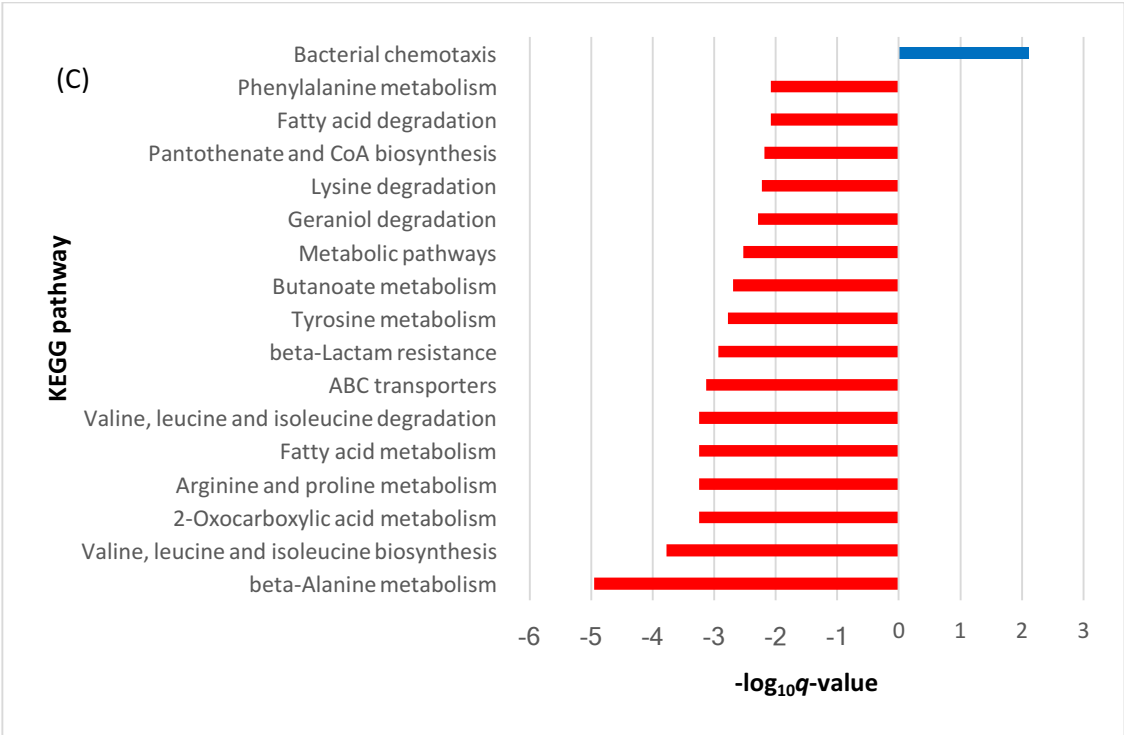

Figure 7: KEGG pathways enriched in (A) Δ*halR*::KanR mutant in early exponential phase, (B) Δ*halR*::KanR mutant in mid-exponential phase, and (C) Δ*halI*::KanR mutant in mid-exponential phase.

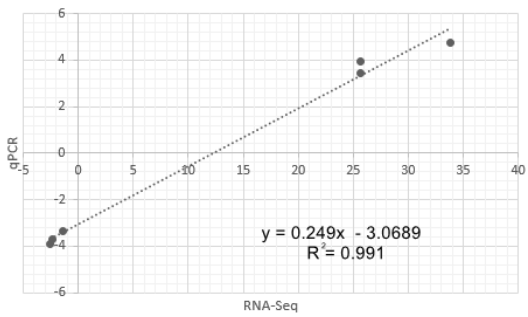

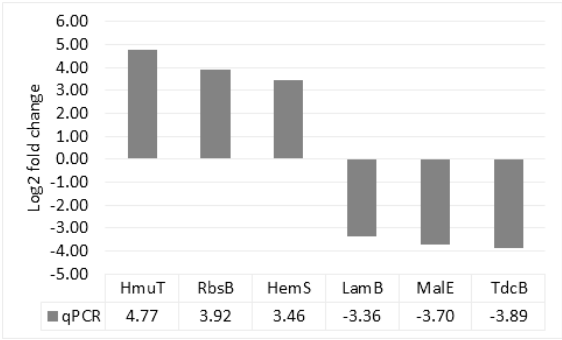

(A) (B)

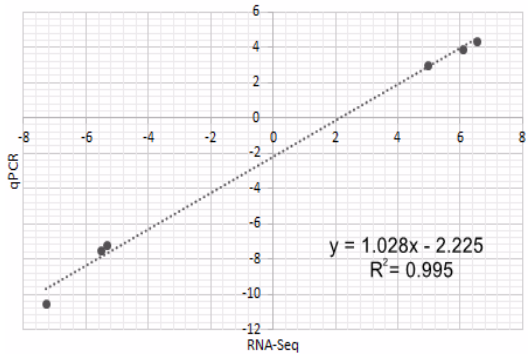

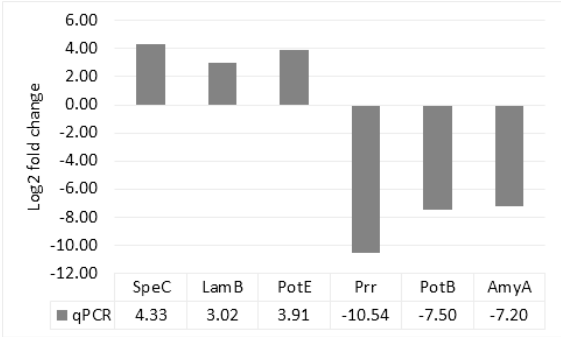

(C) (D)

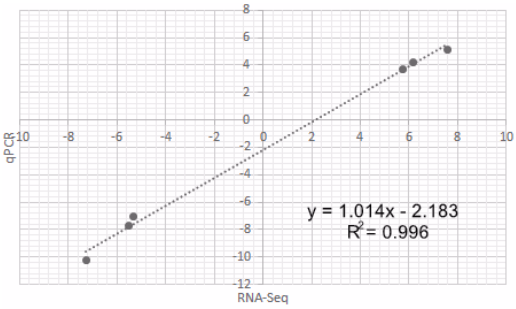

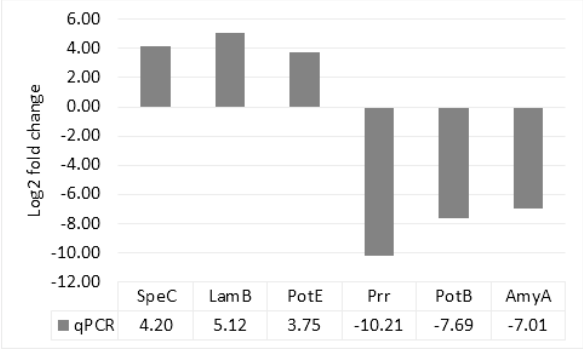

(E) (F)

Figure 8: qPCR validation of RNA-Seq results. Each $\log_2$ ratio of FCs calculated from qPCR was compared with that of the RNA-seq data. (A) Correlation of the FCs between RNA-seq (x-axis) and qPCR (y-axis) of Δ*halR*::KanR in the early exponential phase. (B) Log_2 FCs of Δ*halR*::KanR in the early exponential phase. (C) Correlation of FCs between RNA-seq (x-axis) and qPCR (y-axis) of Δ*halR*::KanR in the mid-exponential phase. (D) Log_2 FCs of Δ*halR*::KanR in the mid-exponential phase. (E) Correlation of fold changes between RNA-seq (x-axis) and qPCR (y-axis) of Δ*halI*::KanR in the mid-exponential phase. (F) Log_2 FCs of Δ*halI*::KanR in the mid-exponential phase.